PERGAMON

Journal of Atmospheric and Solar-Terrestrial Physics 65 (2003) 1021–1033

Journal of ATMOSPHERIC AND SOLAR-TERRESTRIAL PHYSICS

www.elsevier.com/locate/jastp

Time evolution of cosmic-ray intensity and solar flare index at the maximum phase of cycles 21 and 22

H. Mavromichalaki[a,*], P. Preka-Papadema[b], B. Petropoulos[c], A. Vassilaki[a], I. Tsagouri[a]

[a] *Nuclear and Particle Physics Section, Physics Department, University of Athens, Panepistimiopolis Zografos, 15783 Athens, Greece*
[b] *Section of Astrophysics, Astronomy and Mechanics, Physics Department, University of Athens, Panepistimiopolis Zografos, 15783 Athens, Greece*
[c] *Research Center for Astronomy and Applied Mathematics, Academy of Athens, 14 Anagnostopoulou str., 10673 Athens, Greece*

Received 4 April 2002; received in revised form 2 April 2003; accepted 10 May 2003

Abstract

Analysis of the time series into trigonometric series allows the investigation of cosmic-ray (CR) intensity variations in a range of periodicities from a few days to 1 year. By this technique the amplitude and the phase of all observed fluctuations can be given. For this purpose, daily CR intensity values recorded at Climax Neutron Monitor station for the time intervals 1979–1982 and 1989–1991, which correspond to the epochs of maximum activity for solar cycles 21 and 22, respectively, have been studied. The data analysis revealed the occurrence of new periodicities, common or not, in the two solar maxima. A search of our results was done by a power spectral analysis determining independently possible systematic periodic or quasi-periodic variations. Based on the fact that during these maxima the CR intensity tracks the solar flare index better than the sunspot number, the same analysis was performed on these data, which are equivalent to the total energy emitted by the solar flares. Both analyses result in periodicities with different probability of occurrence in different epochs. Occurrence at peaks of 70, 56, 35, 27, 21 and 14- days were observed in all time series, while the periods of 140–154 and 105 days are reported only in the 21st solar maximum and are of particular importance. All of the short-term periods except of those at 27 and 154-days are recorded for first time in CR data, but they had already been observed in the solar activity parameters. Moreover, each parameter studied here has a very different power spectrum distribution in periods larger than 154 days. The possible origin of the observed variations in terms of the CR interaction in the upper atmosphere and the solar cavity dynamics is also discussed here.

Keywords: Galactic cosmic-rays variations; Solar flares; Periodic terms; Neutron Monitors; Solar cycles

1. Introduction

Many authors have reported periodicity in the different kinds of the solar activity from time to time. The observed fluctuations seem to depend on the phase of the solar cycle and the time resolution of the observations. While the 11-year cycle and the 27-day rotational periodicities are the most significant (Watari, 1996), some other periodicities, like these of 300, 150, 74, 51 and 14 days have been recently reported for different indices of solar activity (Bouwer, 1992; Ozgüc and Atac, 1994; Das et al., 1996; Das and Nag, 1999; among others). Most of the studies suggest that there is a periodicity near 154-days (ranging from 152 to 158-days) in occurrence rates of energetic phenomena associated with solar flares. This periodicity was first found in gamma-ray and soft X-ray flares during the time interval 1980–1983 by Rieger et al. (1984) and it seems to be dominant only in cycle 21, especially during the time period of the solar activity maximum from 1978 to 1983.

On the other hand, the analysis of the CR intensity temporal evolution has showed several periodicities, most of

* Corresponding author. Fax: +30-1-7276987.
E-mail address: emavromi@cc.uoa.gr (H. Mavromichalaki).

1364-6826/$ - see front matter © 2003 Elsevier Ltd. All rights reserved.
doi:10.1016/S1364-6826(03)00148-2

which are correlated with solar phenomena. Kudela et al. (1991) studied the frequency distribution of the CR fluctuations and they found a relationship between the general characteristics of power spectral density of CR flux and the random component of the IMF with an indication of a change below 5×10^{-7} Hz (20 months). They noted that there are two distinct parts of CR periodicities, caused by different mechanisms. The large-scale variations (greater than 20 months) are caused by the solar cavity dynamics, whereas the short-scale ones (less than 20 months) are caused by transient effects in interplanetary space. The short-time periodicities have different probability of occurrence in different epochs (Xanthakis et al., 1989). Valdes-Galicia et al. (1996) reported on a newly found 1.68 year variation in the CR intensity, which seems to be correlated with solar X-ray events of long duration and low-latitude coronal hole area variations. They also showed that both 1.68-year and 154-days periodicities in CR intensity are more apparent in cycle 21 than in cycle 20. Valdes-Galicia and Mendoza (1998) proposed that the 154-day periodicity might appear as a consequence of phenomena rooted in the solar interior and it could help in understanding the origin of the solar magnetic cycle. They found that the hard X-ray flares affected the CR modulation more than the sunspot number does during the cycle 21. In a recent work Mavromichalaki et al. (2001) found common periodicities of 140–154, 100, 70, 40–50, 27, 14–16 and 7 days for the galactic CR intensities measured by Neutron Monitor stations and the fluence of solar X-ray flares with energy higher than 50 and 150 keV recorded by Venera-13 and -14 spacecraft during the period 1981–1983. These results are indicative of the close connection between the solar activity and some of the variations in the CR intensity shorter than 1 year. Recently, Kudela et al. (2002) reported on the contributions of three quasi-periodic CR signals ($\sim$ 150 days, $\sim$ 1.3 years and $\sim$1.7 years) in the long time series of daily means of CR intensity observed by four Neutron Monitors during the time interval 1953–2000.

In the present work we investigate the spectral characteristics of the daily values of CR measured at Climax Neutron Monitor station and of the solar flare index (SFI), which is equivalent to the total energy emitted by the flares. The purpose of these analyses is to determine possible similar variations during the maximum phase of the solar cycles 21 and 22. The presence of common periodicities in solar activity indices and CR intensity may help to establish whether there is a relationship between variations in solar activity levels (using the flare index as a proxy) and CR modulation.

2. Method of analysis and results

The time profiles of monthly mean values of the SFI and the sunspot number during the solar cycles 21 and 22 are different, as it is shown in the upper and middle panels of Fig. 1. The sunspot number maximum of the cycle 21 was

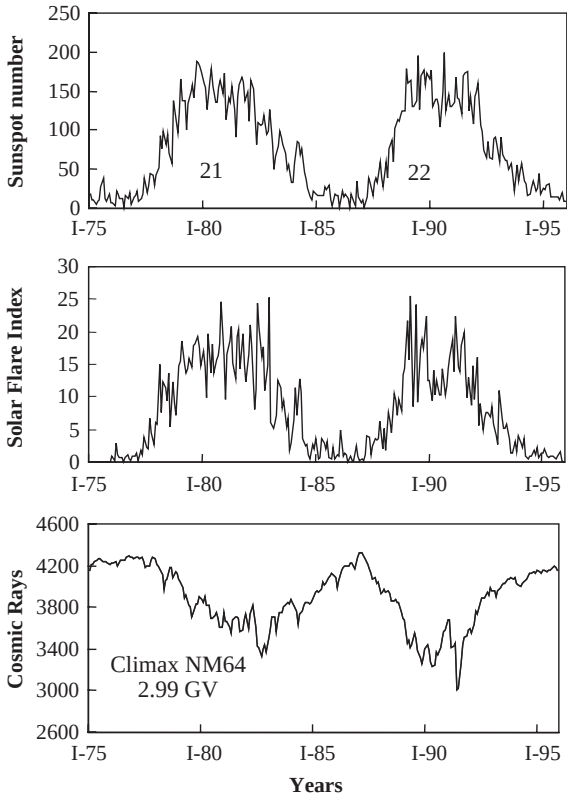

Fig. 1. Monthly mean values of the sunspot number and SFI (upper two panels) as well as of the CR intensity of Climax Neutron Monitor Station (lower panel) for the period 1975–1995 (cycles 21 and 22).

occurred at the year 1980, about 2 years before the SFI maximum, which is recorded at the year 1982. On the other hand, during the cycle 22 there are two maxima in SFI data at the years 1989 and 1991, respectively, in coincidence with the sunspot number maximum. It is noteworthy that the CR intensity shown in the lower panel of the same figure follows more closely the behavior of SFI than the sunspot number. It seems to be that the CR intensity is a mirror image of the SFI, as well as of the interplanetary magnetic field according to Cane et al. (1999).

In order to study the temporal evolution of these indices in the solar maxima of cycles 21 and 22, daily values of CR intensity recorded by the Climax Neutron Monitor Station (cut-off rigidity 2.99 GV) and of the SFI during the time intervals 1979–1982 and 1989–1991 (Solar Geophysical Data, 1997) were used. The SFI quantifies the daily flare activity for the full disk of the Sun over 24 h per day, and it is calculated by the formula $Q = it$, where i is the importance coefficient of the flare and t is the duration of the flare in minutes (Ozgüc and Atac, 1994). The identification of common variations in both data sets might help to understand the relationship between the evolution of

solar activity, solar flares, photospheric fields, open magnetic flux and the heliospheric magnetic field.

2.1. Successive approximations method

By applying the technique of detrending time series by trigonometric series we investigated the CR intensity and SFI variations in a wide periodicity range corresponding from 14 days to 1 year. According to the technique of successive approximations (SA) the amplitude and the position of these variations are computed and are expressed analytically. This method has been introduced by Xanthakis et al. (1989) to study CR time series from various Neutron Monitor stations. Several periodical sinusoidal waves are applied on the observed time series to reproduce them. The amplitude and phases of these waves are obtained by successive fittings on the data set. It can also be used to non-continuous functions. An appropriate software for the application of the SA method to the time series have been developed at first by Liritzis et al. (1999) and it is used in the present study.

The basic idea of the method is to derive the best fitted trigonometric series to the observed ones in order to find, at first, long-term variations and to express them analytically according to the following relation:

$$A^{\mathrm{cal}} = a_0 + \sum_{i=1}^{n} a_i \sin[(2\pi/T_i)(T - T_s)], \tag{1}$$

where A^{cal} in our case can be the calculated CR intensity (C^{cal}) or the SFI (I^{cal}) accordingly, T_s, T_e are the start- and the end-time of each estimated quasi-periodicity T, a_0 is the constant shift of the curve, a_i is the amplitude of the i-sinusoidal wave (positive or negative value means that it is up or down to the constant shift). T_i is the ith quasi-periodicity.

In the next steps, the difference between the observed (A^{obs}) and calculated by Eq. (1) values (residuals) is fitted by a similar relation in order to identify smaller variations and reproduce the observed time series with the best approximation. The accuracy of the computations (A_c) and the degrees of freedom (F) are checked step by step, suggesting that the parameters used in these expressions would be less than the number of measurements. The standard deviation (σ) and the corresponding accuracy (A_c) between the observed and calculated values are estimated by the relations:

$$\sigma = \sqrt{\frac{\sum (A^{\mathrm{obs}} - A^{\mathrm{cal}})^2}{N-1}}, \tag{2}$$

$$A_c = 1 - \frac{\sigma}{\langle x \rangle}, \tag{3}$$

where N is the number of data points and $\langle x \rangle$ is the mean number of data per time interval.

Successive results from the application of this technique on the SFI and CR time series, during the solar maxima 21 and 22, are illustrated in Figs. 2a and b and Figs. 3a and b, respectively. The analytical expressions for both time series and the calculated amplitude and phase of each variation are given in Tables 1–4. A satisfactory agreement between the observed and the calculated values is resulted from these figures, as it is also confirmed from the standard deviation (and the accuracy) between observed and calculated values.

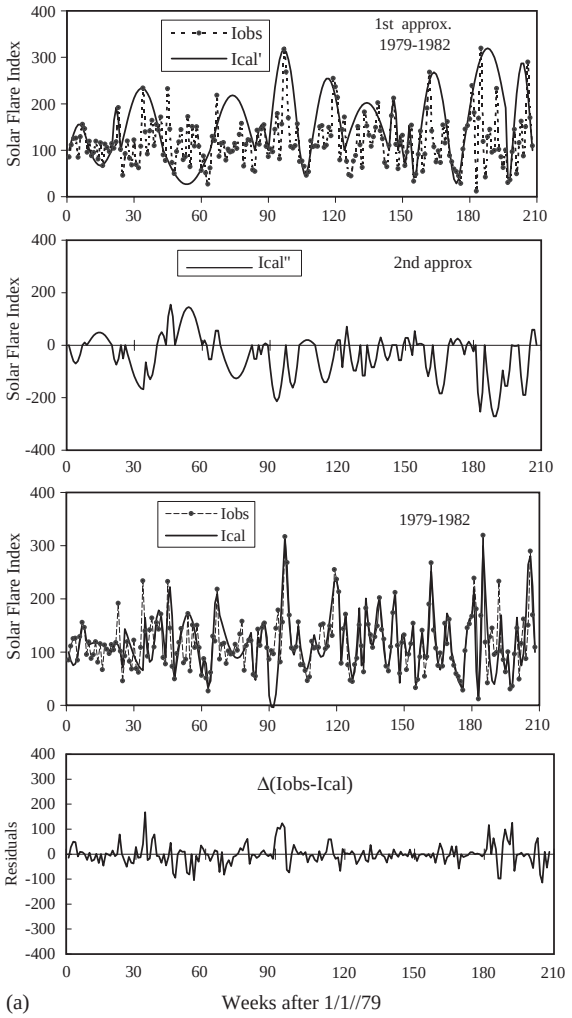

Fig. 2. (a) Graphic presentation of the SFI time series for the interval 1979–1982. The top panel gives the first fitting ($I_{\mathrm{cal}'}$) to the observed data series (I_{obs}). The second one gives the second approximation ($I_{\mathrm{cal}''}$). The next panel gives the observed (I_{obs}) and the calculated by the expressions of the Table 1 (I_{cal}) values of SFI. The residuals between observed and calculated values Δ (I_{obs}–I_{cal}) are presented in the bottom panel ($A_c = 66\%$). (b) Graphic presentation of the CR intensity series for the interval 1979–1982. The top panel gives the first fitting ($C_{\mathrm{cal}'}$) to the observed data series (C_{obs}). The second one gives the second approximation ($C_{\mathrm{cal}''}$). The next panel gives the observed (C_{obs}) and the calculated by the expressions of the Table 2 (C_{cal}) values of the CR intensity. The residuals between observed and calculated values Δ (C_{obs}–C_{cal}) are presented in the bottom panel ($A_c = 96\%$).

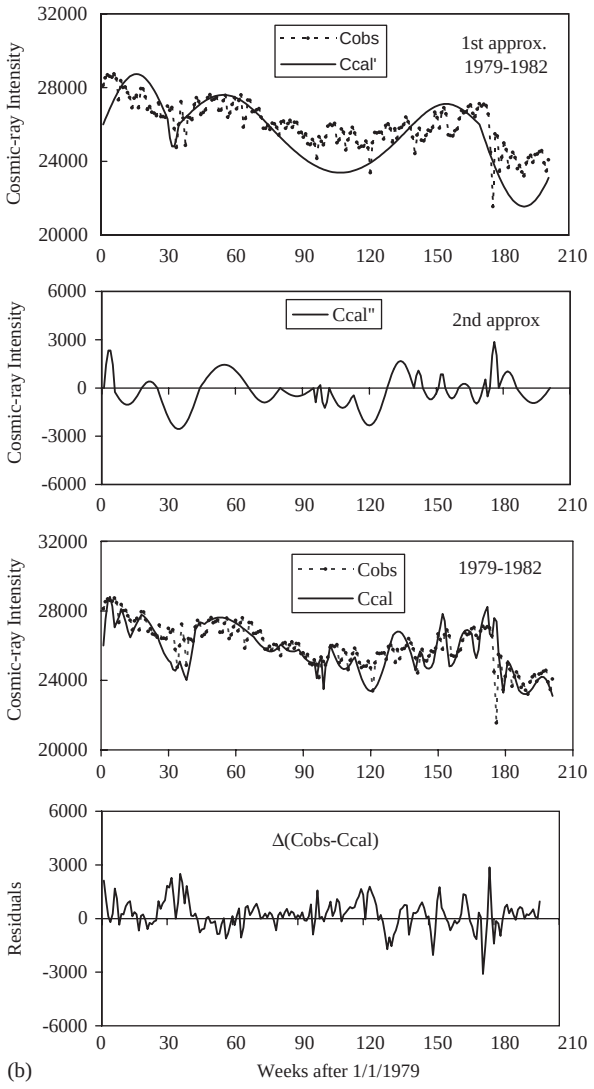

Fig. 2. *continued.*

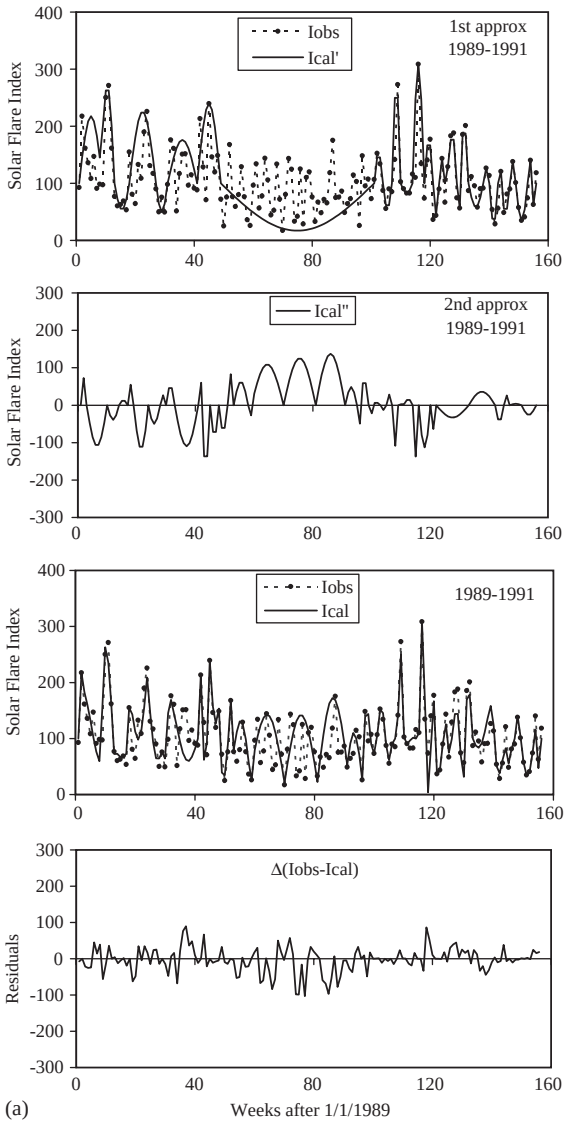

Fig. 3. (a) Graphic presentation of the SFI time series for the interval 1989–1991. The top panel gives the first fitting ($I_{cal'}$) to the observed data series (I_{obs}). The second one gives the second approximation ($I_{cal''}$). The next panel gives the observed (I_{obs}) and the calculated by the expressions of the Table 3 (I_{cal}) values of SFI. The residuals between observed and calculated values Δ (I_{obs}–I_{cal}) are presented in the bottom panel ($A_c = 68\%$). (b) Graphic presentation of the CR intensity series for the interval 1989–1991. The top panel gives the first fitting ($C_{cal'}$) to the observed data series (C_{obs}). The second one gives the second approximation ($C_{cal''}$). The next panel gives the observed (C_{obs}) and the calculated by the expressions of the Table 4 (C_{cal}) values of the CR intensity. The residuals between observed and calculated values Δ (C_{obs}–C_{cal}) are presented in the bottom panel ($A_c = 98\%$).

Specifically, occurrences at peaks of 154, 140, 105, 70, 35, 27, 21 and 14 days were found out at the observed SFI time series for the time interval 1979–1982 and are presented in the upper panel of Fig. 2a. The standard deviation (σ) is equal to 85.705, and the accuracy (A_c) is 47%. In a second step, new trigonometric series were fitted to the residuals and occurrences at 105, 70, 56, 35, 27, 21 and 14 days were recorded (second panel of Fig. 2a). Summarizing the results from all the steps, the calculated time series together with the observed ones as well as the final residuals are given in the two lower panels of Fig. 2a. The standard deviation is 40.931 with 50 degrees of freedom, while the accuracy (A_c) is up to 66%.

In a similar way, peaks at 462, 280, 210 and 35 days with $A_c = 95\%$ appeared in the observed CR data during

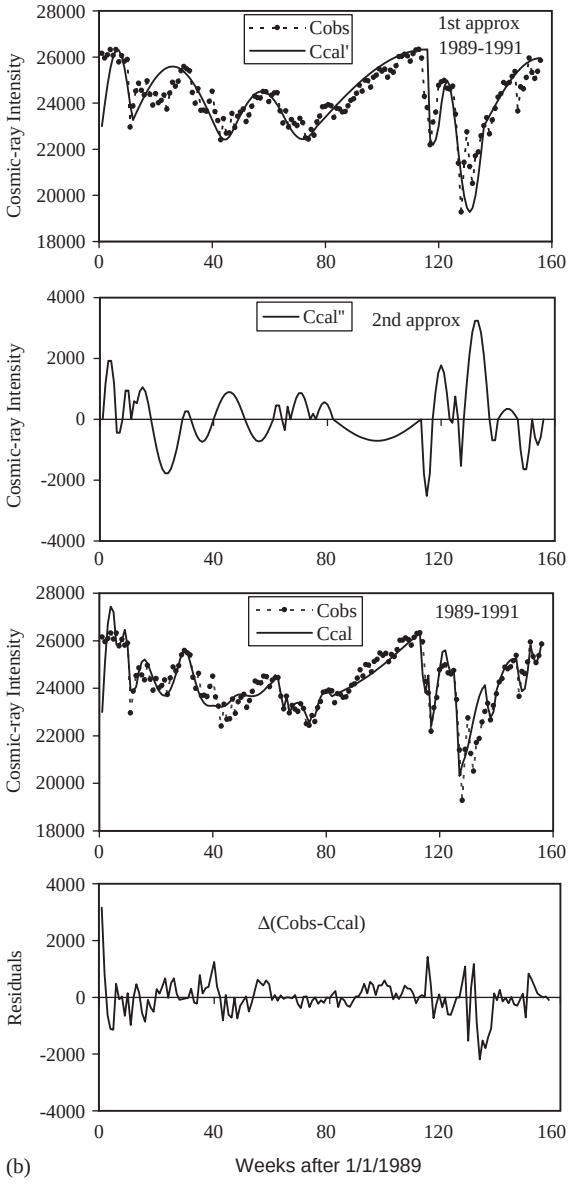

Fig. 3. *continued.*

the 21st solar maximum in the first approximation, as it is shown in the upper panel of Fig. 2b. The final calculated time series comparing with the observed one as well as the final residuals are given in the two lower panels of the same figure. Peaks at 462, 280, 238, 210, 154, 140, 126, 105, 70, 56, 35, 28, 21 and 14 days are finally obtained from this analysis with an accuracy up to 96%.

During the maximum phase of the solar cycle 22, the same analysis was performed on the SFI and CR time series (see Figs. 3a and b and Tables 3 and 4). The periods of 364, 70, 56, 35, 28, 21 and 14 days were obtained by the first approximation ($A_c = 51\%$, $\sigma = 51.052$) and those of 70, 56, 35, 28, 21 and 14 days by the second approximation for the SFI time series ($A_c = 68\%$, $\sigma = 34.306$ and $F = 4$). In the CR time series, the quasi-periodical terms of 546, 280, 210, 140, 70, 56, 35 and 28 days were obtained by the first approximation ($A_c = 97\%$, $\sigma = 800.942$), and the ones of 210, 70, 56, 35, 28, 21 and 14 days by the second approximation ($A_c = 98\%$, $\sigma = 592.265$ and $F = 60$).

The synoptic results of the SA analysis on the SFI and CR time series during the 21st and 22nd solar maximum are given in Table 5. The number of appearance of each variation in any time series is presented next to it. We note that the terms 546 and 462 days expressing a trend of the corresponding time series, are given in parentheses, while the periodicity of 14 days is near to the Niquist point. The occurrences of 70, 56, 35, 28, 21 and 14 days obtained in both time series (CR and SFI) for the two solar maxima. However, occurrences at peaks of 140 and 154 days appeared in CR and SFI data only in the maximum phase of the solar cycle 21. The last result holds also for the peak of 105 days, while the one of 126 days was only found in the CR data. The periodical term of 140 days that was appeared only once in the CR time series during the 22nd solar maximum, cannot constitute a strong evidence of the periodicity of 140 days in the above time series. The fluctuations of 210 and 280 days were obtained in both CR time series corresponding to both solar maxima, while the peak at 238 days is only appeared in the CR data for the maximum of the cycle 21. In addition, the variation of 365 days was also found in SFI data at the maximum phase of cycle 22.

2.2. Power spectrum analysis

Moreover, in order to verify possible systematic periodic or quasi-periodic variations obtained by the method of the successive approximations in the different residuals, a Blackman and Tukey (1959) power spectrum analysis (PSA) was carried out in the CR intensity and SFI data. The obtained power spectra were derived from autocorrelation functions that were truncated at various lags. The frequency band is determined by the maximum phase lag points, which give the spectrum bandwidth. In most of the cases, the maximum phase lag is chosen to be equal to the 1/3 of the number of data sample. The equivalent degrees of freedom (edf) are computed by the formula $\text{edf} = 2Bn/m$, where B is the standardized bandwidth of the spectrum (in our case $B = 1$), n is the number of data points and m is the maximum phase lag. If the maximum phase lag is quite large (not larger than $n/3$) the spectrum is appeared with much more peaks (fluctuations). In the opposite case (small lag) the spectrum is appeared with much less fluctuations.

The PSA is a well-established statistical method that is based on the estimation of the significant periods over several confidence levels according to an x^2 distribution. For this purpose, the spectral estimates and the red noise curve, corresponding to the background level is computed for every frequency. The confidence levels are computed

Table 1
Analytical expression of the SFI as a function of quasi-periods (in days) for the time interval 1979–1982
$I^{cal} = 100 + a_1 \sin[(2\pi/154)(T-T_s)] + a_2 \sin[(2\pi/140)(T-T_s)] + a_3 \sin[(2\pi/105)(T-T_s)] + a_4 \sin[(2\pi/70)(T-T_s)] + a_5 \sin[(2\pi/56)(T-T_s)] + a_6 \sin[(2\pi/35)(T-T_s)] + a_7 \sin[(2\pi/28)(T-T_s)] + a_8 \sin[(2\pi/21)(T-T_s)] + a_9 \sin[(2\pi/14)(T-T_s)]$[a]

a_1	219.290	(177–196)
a_2	−73.200	(43–64)
	118.100	(64–84)
	102.020	(124–144)
	133.680	(24–43)
a_3	−167.629	(26–34)
	154.820	(109–124)
	217.040	(90–104)
	167.750	(157–171)
	−126.658	(68–82)
a_4	145.185	(48–60)
	48.940	(9–20)
	−33.110	(10–20)
	55.880	(1–10)
	189.790	(199–208)
	−143.212	(110–119)
	−274.948	(185–192)
a_5	−214.076	(89–97)
	20.350	(103–110)
	−188.774	(162–169)
a_6	54.640	(84–90)
	−71.550	(171–177)
	−70.121	(1–7)
	−130.391	(34–40)
	−161.839	(97–103)
	−53.920	(104–109)
	−101.816	(125–130)
	−88.487	(133–138)
	−163.728	(192–197)
	−199.187	(200–205)
a_7	91.770	(20–24)
	112.160	(144–148)
	−73.920	(20–24)
	49.447	(40–44)
	154.226	(44–48)
	−57.926	(140–144)
	−118.274	(158–162)
	25.680	(171–175)
	−253.778	(181–185)
a_8	−66.950	(154–157)
	−69.580	(196–199)
	−62.290	(62–65)
	64.484	(65–68)
	−60.605	(82–85)
	22.279	(119–121)
	−134.067	(130–133)
	−66.739	(146–149)
	32.130	(149–152)
	6.260	(155–158)
	−3.610	(197–200)
	67.795	(205–208)
a_9	32.130	(148–150)
	−33.080	(150–152)
	54.030	(152–154)
	10.511	(7–9)
	−50.976	(24–26)
	19.240	(60–62)
	34.800	(85–87)
	7.320	(87–89)
	−83.961	(121–123)
	71.130	(123–125)
	29.881	(138–140)
	0.000	(144–146)
	−38.160	(152–153)
	54.030	(153–155)
	24.322	(169–171)
	−35.775	(175–177)
	14.142	(177–179)
	−23.846	(179–181)

[a] $T_s < T < T_e$, where T_s, T_e are given in parentheses next to the corresponding coefficient a_i in weeks after 1/1/79.

by multiplying the red noise curve values by the confidence coefficients which denote that a normally distributed statistic can be found between the limits $\pm 1.96\sigma$, $\pm 2.58\sigma$, etc. (σ is the standard deviation) for the confidence levels of 95%, 99%, etc. If one peak (i.e. spectral estimates value) is larger than the corresponding confidence level value, it is considered as a significant peak and gives a significant frequency or period for this confidence level.

The PSA was performed in all four data series using a 5-day moving average and a time lag equal to 1/3 of the number of data points in order to obtained periodicities in frequency band from 10^{-3} to 10^{-1} c/day. The obtained power

Table 2
Analytical expression of CR intensity as a function of quasi-periods (in days) for the time interval 1979–1982
$C^{cal} = 26,000 + a_1 \sin[(2\pi/462)(T - T_s)] + a_2 \sin[(2\pi/280)(T - T_s)] + a_3 \sin[(2\pi/238)(T - T_s)] + a_4 \sin[(2\pi/210)(T - T_s)] + a_5 \sin[(2\pi/154)(T - T_s)] + a_6 \sin[(2\pi/140)(T - T_s)] + a_7 \sin[(2\pi/126)(T - T_s)] + a_8 \sin[(2\pi/105)(T - T_s)] + a_9 \sin[(2\pi/70)(T - T_s)] + a_{10} \sin[(2\pi/56)(T - T_s)] + a_{11} \sin[(2\pi/35)(T - T_s)] + a_{12} \sin[(2\pi/28)(T - T_s)] + a_{13} \sin[(2\pi/21)(T - T_s)] + a_{14} \sin[(2\pi/14)(T - T_s)]$[a]

a_1	2641.738	(72–138)
	−2614.199	(75–140)
	2623.888	(31–42)
	415.160	(8–18)
a_2	2645.856	(160–201)
	1604.199	(35–75)
	−4449.600	(170–201)
	−1046.945	(18–28)
	982.204	(88–98)
	782.680	(155–165)
a_3	−1373.542	(38–72)
a_4	2735.500	(1–30)
	1115.199	(140–170)
	−1826.114	(1–30)
	1342.656	(42–72)
	−2448.931	(100–130)
	2304.188	(100–130)
a_5	−1702.630	(138–160)
	−1445.981	(46–68)
	1437.891	(44–66)
a_6	1380.108	(130–151)
	1560.235	(181–201)
	699.098	(68–88)
	1064.822	(12–31)
	−2550.646	(25–44)
a_7	−1343.974	(151–169)
	2205.202	(28–46)
	−2367.621	(130–148)
a_8	−940.716	(72–88)
	−2331.832	(112–128)
	−1862.999	(178–193)
	−515.465	(80–95)
	−937.465	(186–201)
	−900.442	(66–80)
a_9	−1046.354	(5–18)
	2498.127	(1–12)
	−2009.878	(88–100)
	−4919.645	(169–181)
	−1241.981	(102–112)
	1679.953	(128–140)
a_{10}	4355.197	(169–178)
	2106.352	(30–38)
	−1695.003	(1–8)
	964.585	(193–201)
	1034.883	(178–186)
	1743.159	(148–155)
	413.210	(18–25)
	−723.379	(144–151)
a_{11}	−657.596	(154–160)
	−977.005	(165–171)
	−1255.500	(30–35)
	2447.611	(1–5)
	273.324	(160–165)
a_{12}	−1110.595	(165–169)
	−1242.953	(98–102)
	1081.267	(140–144)
	2869.764	(174–178)
a_{13}	986.831	(151–154)
	−616.855	(171–174)
a_{14}	−1242.953	(98–100)
	−892.197	(95–97)
	181.333	(97–98)

[a] $T_s < T < T_e$, where T_s, T_e are given in parentheses next to the corresponding coefficient a_i in weeks after 1/1/79.

spectra by all the examined time series are illustrated in Fig. 4. The red noise curve and the confidence levels of 95% up to 99% are shown in each panel of this figure. A set of well determined periodicities was found at confidence levels of 95% up to 99% (Table 6). We note that the long-term periodicities are not clearly shown in this figure due to the selected frequency scale.

The periodicity of 48–56 days, as well as the well-known rotational periodicity of 27 days are appeared in all time series during both time intervals. The periodicities of 37, 21, 14 and 10 days in the CR data and the ones of 75 and 5 days in the SFI data are obtained during both solar maxima. The periodicity of 140 days in the CR time series (using the time lag = 73 corresponding to $n/20$) and the SFI time

Table 3
Analytical expression of SFI as a function of quasi-periods (in days) for the time interval 1989–1991
$I^{cal} = 100 + a_1 \sin[(2\pi/364)(T - T_s)] + a_2 \sin[(2\pi/70)(T - T_s)] + a_3 \sin[(2\pi/56)(T - T_s)] + a_4 \sin[(2\pi/35)(T - T_s)] + a_5 \sin[(2\pi/28)(T - T_s)] + a_6 \sin[(2\pi/21)(T - T_s)] + a_7 \sin[(2\pi/14)(T - T_s)]$[a]

a_1	−82.880	(49–101)
a_2	109.318	(59–70)
	125.112	(70–81)
	−33.180	(122–133)
	76.140	(31–41)
	137.477	(81–91)
	125.930	(18–27)
	36.397	(133–142)
a_3	117.530	(1–8)
	139.490	(41–49)
	−110.039	(33–41)
	−109.210	(3–10)
a_4	171.260	(8–13)
	−46.510	(13–18)
	−42.120	(133–138)
	−116.776	(19–24)
	63.055	(53–58)
	−26.000	(151–156)
a_5	50.670	(27–31)
	−17.240	(110–114)
	208.590	(114–118)
	−65.050	(149–153)
	−38.914	(10–14)
	−50.086	(24–28)
	48.595	(91–95)
	−112.955	(116–120)
	3.677	(147–151)
a_6	52.540	(101–104)
	−44.330	(104–107)
	173.090	(107–110)
	77.080	(118–121)
	88.400	(126–129)
	101.080	(130–133)
	−71.470	(140–143)
	−51.490	(144–147)
	13.144	(14–17)
	52.611	(30–33)
	−157.952	(42–45)
	−82.782	(45–48)
	−70.066	(48–51)
	67.924	(96–99)
	7.039	(100–103)
	2.851	(109–111)
	15.900	(111–114)
	−43.960	(142–145)
a_7	−56.440	(121–123)
	43.480	(123–125)
	29.180	(125–126)
	−43.450	(129–130)
	26.620	(138–140)
	20.950	(143–144)
	37.860	(147–149)
	40.350	(153–154)
	−37.380	(154–156)
	72.553	(1–3)
	54.860	(17–19)
	26.510	(28–30)
	60.139	(41–42)
	82.679	(51–53)
	−26.929	(58–59)
	−49.473	(95–96)
	−21.966	(99–100)
	−12.650	(103–105)
	28.451	(105–107)
	−108.470	(107–109)
	−137.235	(114–116)
	−63.410	(120–122)
	25.812	(145–147)

[a] $T_s < T < T_e$, where T_s, T_e are given in parentheses next to the corresponding coefficient a_i in weeks after 1/1/89.

Table 4
Analytical expression of CR intensity as a function of quasi-periods (in days) for the time interval 1989–1991
$C^{cal} = 23,000 + a_1 \sin[(2\pi/546)(T - T_s)] + a_2 \sin[(2\pi/280)(T - T_s)] + a_3 \sin[(2\pi/210)(T - T_s)] + a_4 \sin[(2\pi/140)(T - T_s)] + a_5 \sin[(2\pi/70)(T - T_s)] + a_6 \sin[(2\pi/56)(T - T_s)] + a_7 \sin[(2\pi/35)(T - T_s)] + a_8 \sin[(2\pi/28)(T - T_s)] + a_9 \sin[(2\pi/21)(T - T_s)] + a_{10} \sin[(2\pi/14)(T - T_s)]$[a]

a_1	3330.699	(77–116)
a_2	2950.400	(136–156)
a_3	−702.474	(82–113)
	2589.500	(11–41)
a_4	1503.500	(48–67)
a_5	3324.600	(1–11)
	−1795.913	(18–29)
	900.292	(40–51)
	−567.199	(67–77)
	−3724.400	(126–136)
	−732.168	(51–61)
	3294.115	(128–137)
a_6	−741.114	(32–40)
	−590.600	(41–48)
	881.739	(67–74)
	347.320	(140–147)
a_7	1981.600	(120–126)
	1056.900	(12–18)
	567.590	(76–82)
	1773.000	(117–123)
	2022.852	(1–5)
	−1731.824	(147–152)
a_8	−811.699	(116–120)
	−2522.699	(113–117)
	−844.275	(152–156)
a_9	−510.459	(5–8)
	1095.986	(8–11)
	305.150	(29–32)
	523.832	(61–64)
	−794.445	(137–140)
a_{10}	600.523	(11–12)
	−354.986	(64–65)
	415.032	(65–67)
	186.792	(74–76)
	−114.916	(123–124)
	750.300	(124–126)
	−1535.253	(126–128)

[a] $T_s < T < T_e$, where T_s, T_e are given in parentheses next to the corresponding coefficient a_i in weeks after 1/1/89.

series, extending to the 162 days (near to 154 days) in the last one, are only found during the 21st solar maximum. On the other hand, the periodicity of 365 days is only obtained for CR and SFI data during 22nd solar maximum. We note that terms greater than 365 days are expressing a trend of these time series.

3. Discussion

The spectral analysis of daily values of CR intensity at Neutron Monitor Station of Climax and the SFI in the frequency range 10^{-9}–10^{-7} Hz, permitted us to present a comprehensive description of the behavior of spectral density distribution in a range of periodicities from 14 days to 1 year, during the maxima of solar cycles 21 and 22. Two methods of analysis, SA and PSA, were used in order to find periodic variations common or not between CR and SFI time series (Tables 5 and 6). The SA method of analysis gives the opportunity to define the amplitude and the phase of the observed variations as well as the analytical expression that 'reproduces' the observed time series (Tables 1–4).

It is concluded that a network of short-term peaks in SA analysis smaller than 70 days occurred in all time series, included the well-known periodicity of 27 days due to the solar rotation. The peaks of 14, 27, 35, 56 and 70–75 days were appeared in all the time series, whereas the one of 21 days was found in the CR time series during the two solar maxima according to both methods of analysis. Moreover, the existence of the periods at 105 and 126 days seem to be different in each data set, although the period of 105 days is prominent in the 21st solar maximum in solar activity and CR intensity.

The 27-day synodic period is well-established main periodicity of solar activity and the related solar output. The existence of this recurrence in CR data is accepted as a good indicator of the global sectorial pattern of heliospheric magnetic fields (Antalova et al., 2001).

Table 5
Results of the successive approximation method on the CR and SFI data series for the 21st and 22nd solar maxima (in days)

CR (1979–1982)	SFI (1979–1982)	CR (1989–1991)	SFI (1989–1991)
—	—	(546) (1)	—
(462) (2)	—	—	—
—	—	—	364 (1)
280 (3)	—	280 (1)	—
238 (1)	—	—	—
210 (6)	—	210 (2)	—
154 (3)	154 (1)	—	—
140 (5)	140 (4)	140 (1)	—
126 (3)	—	—	—
105 (6)	105 (5)	—	—
70 (11)	70 (7)	70 (7)	70 (7)
56 (8)	56 (3)	56 (4)	56 (4)
35 (5)	35 (10)	35 (6)	35 (6)
28 (4)	28 (9)	28 (3)	28 (9)
21 (2)	21 (12)	21 (5)	21 (18)
14 (3)	14 (18)	14 (7)	14 (23)

Note: The number of appearance of each periodicity is given in parentheses.

The other peaks of 35, 21, 14 and 10 days occurred in both solar maxima give evidence for an attribution to the CR variations of the solar induced effects to the interplanetary medium. Valdes-Galicia et al. (1999) found significant peaks in different Neutron Monitor data during the declining phase of cycle 22 suggesting that some of them are rigidity dependent fluctuations. The obtained periodicities around 105, 70, 21 and 14 days are close to our results. They noted that sunspot monthly averages do not show the periodicities that are found in CR data except the one of the 27 days, which is associated to the solar rotation. They concluded that it would be useful to look for other manifestations of solar activity to attribute the observed CR fluctuations.

The peaks of the spectral estimates at 70–75 and 56 days seem to be common periodicities in CR and SFI data sets for the two solar maxima. Ozgüc and Atac (1994) have already reported the periodicities of 52 and 75 days in SFI time series during the time interval 1988–1991. Bai (1994) reported that beside the 154-day variation, periodicities of 51, 78, 104 and 129 days are often detected in solar activity and these periods are very close to integrated multiples (2, 3, 4, 5, 6) of 25.5 days. These periodicities are not continuously in operation, but they are rather episodic in nature.

The most interesting result of this analysis is that the CR and SFI period of 140–154 days is prominent in the 21st solar maximum. This periodicity has previously been reported in both CR data (Valdes-Galicia et al., 1996; Kudela et al., 2002) and flare-related data by many authors for different time intervals (e.g. Rieger et al., 1984; Bai and Cliver, 1990; Verma et al., 1992, etc). Ozguc and Atac (1989) reported this periodicity in SFI time series during the time interval 1966–1986. Wolff (1992) interpreted this periodic behavior to periodic sources located in the solar interior caused by global oscillation modes. Bai and Cliver (1990) underlined that there are cases where a periodicity is seen to disappear for a long interval and then to appear at the same phase or 180° out of space and an example of this effect is the 155-day periodicity. Recently, Kudela et al. (2002) presented wavelet transform results from the time series of daily averages of the nucleonic intensity recorded by NMs at four different cut-off rigidities over a period of four solar cycles and described the PSD temporal evolution at the periodicities of 150–160 days, $\sim$ 1.3 years and $\sim$ 1.7 years. They indicated that the quasi-periodicity of about 150 days is not stable and it ranges from 140 days to more than 200 days appearing usually just after the solar maxima. Consistently with this indication, this periodicity is appeared only in the 21st solar maximum (odd cycle) and not in the 22nd (even cycle). Moreover, the structure of two discrete periodicities of 140 and 154 days of solar origin determined from the SFI data and a new one of 210 days appeared only in CR data series. The same result has been reported by Kudela et al. (2002) for the 1.7 year periodicity in CRs which was more dominant in the odd cycle 21 and not in the cycles before and after it (cycles 20 and 22). Rybak et al. (2000) as well as Antalova et al. (2000) remarked the intermittent character of the 150-day solar periodicity in the 20, 21 and 22 cycles for solar soft X-ray parameters, while the power of the 155-day periodicity of solar SXR data is remarkably better during the 21st than in the 20th cycle. Cane et al. (1998) found that the IMF power average in 1978–1982 was larger than in 1968–1972 for 150-days periodicity.

Furthermore, the variations of 210 and 280 days were found in CR time series for both solar maxima and the one of 238 days, for the 21st solar maximum. The corresponding values by using the PSA method are the periodicities of 182 and 242 days but only for the 22nd solar maximum, while the fluctuation of 1 year is obtained in SFI time series during the 22nd solar maximum. It is noted that periods of 180 and 240 days have been also found in Neutron Monitor data for the period 1964–1985 by Xanthakis et al. (1989). Okhlopkov et al. (1986) reported on the annual CR variation, as well as on periods of 274 and 183 days, in the low atmosphere based on CR measurements by using sounding balloons over the period 1958–1980.

The SA power peak around 462 days (1.3 year) period was only appeared in CR data in the time interval 1979–1982. Rybak et al. (2001) demonstrated this peak in the Magnetic Plage Strength Index in 1980 and 1982 and somewhat less prominent in the years 1991 and 1992, while in CR data of the years 1980 and 1991 the wavelet power spectrum shows the 475-days period well defined.

We note that according to our knowledge periodicities of 35, 56, 70 and 210 days are indicated for first time in CR data. Surely these periodicities are rigidity dependent and a further investigation with the examination of CR data from more Neutron Monitor stations will be helpful in this

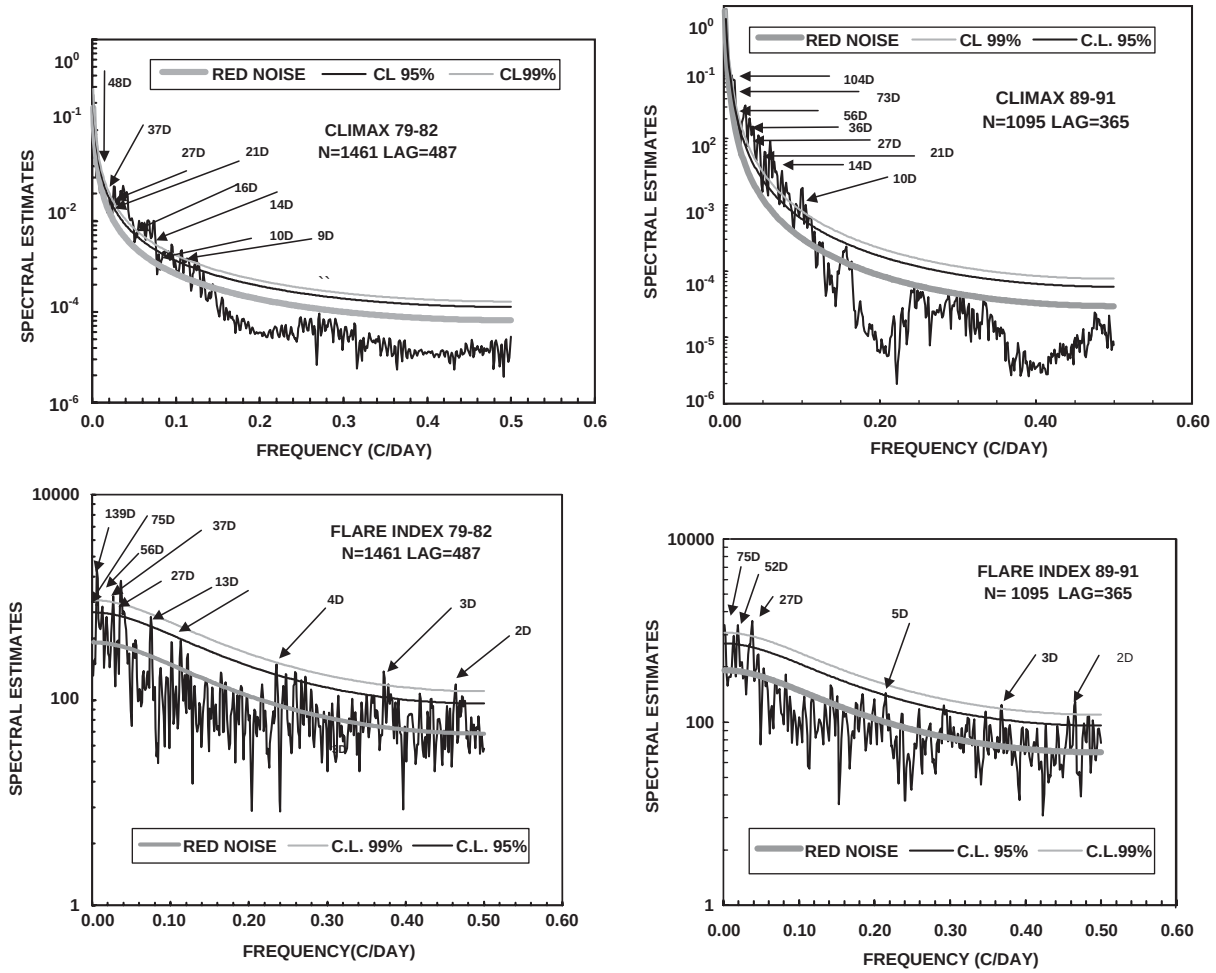

Fig. 4. PSA of daily values of CR intensity (upper panels) and SFI (lower panels) time series for the intervals 1979–1982 and 1989–1991, respectively. Peaks with confidence level greater than 95% are also indicated.

direction. On the other hand, some peaks as those of 14, 27, 35, 105 and 365 days reported in SFI data are also newly found.

4. Conclusions

Summarizing we can say that spectral characteristics of CR intensity and the solar flare index (SFI) time series seem to be different from cycle to cycle (even or odd) and depend on the phase of the cycle and on the data sets under study. Similar periodicities observed in both time series during the cycle maxima give evidence that short-term periodicities, ranging from 14 days to 365 days, in CR intensity are not always caused by transient effects in the interplanetary medium. They are rather attributed to the solar cavity dynamics as the long-term ones. Consistent conclusions have also been reported by Valdes-Galicia and Mendoza (1998), Valdes-Galicia et al. (1999). Recently, Yu-Qing (2002) reported that Rossby and mixed Rossby–Poincare waves induced periods of 155, 126, 102, 76–78 and 51–54 days in flare activities and sunspot areas or groups during solar maxima. It is reported that notable periods during maxima of different solar cycles from various data sets are that of 154, 128, 102, 78 and 51 days. The problem of the origin of such quasi-periodicities particularly prominent during solar maxima remained unsolved for many years.

If alternative periodicities are a systematic feature of the consecutive cycles, it implies the relevance of the identified differences between even and odd solar activity cycles (Mavromichalaki et al., 1988, 1997). Although a strong evidence for the above result is that the periodicity of 154 days was found in SFI and CR data only in the 21st cycle, more work is needed on the subject, because it is not straightforward to relate CRs variability directly to the solar

Table 6
Results of the PSA on the CR and SFI data series for the 21st and 22nd solar maxima (in days)

CR (1979–1982) lag = 487	SFI (1979–1982) lag = 487	CR (1989–1991) lag = 365	SFI (1989–1991) lag = 365
			730* (> 99%)
		363* (> 95%)	365* (> 94%)
		242* (> 99%)	
	195* (> 95%)	182* (> 95%)	
	162* (> 99%)		
140 (lag = 73) (> 99%)	139 (> 99%)		
		104 (> 99%)	
	75 (> 95%)	73 (> 99%)	75 (99%)
48 (> 95%)	56 (95%)	56 (> 95%)	52 (99%)
37 (> 99%)	37 (> 99%)	36 (> 99%)	
27 (> 99%)	27 (> 99%)	27 (> 99%)	27 (> 99%)
21 (> 99%)		21 (> 99%)	
		19 (> 99%)	
16 (> 99%)		17 (> 99%)	
14 (> 99%)	13 (> 95%)	14, 13 (> 99%)	
10, 9 (> 99%)		10 (> 99%)	
	4 (> 99%)		5 (> 95%)
	3 (> 99%)		3 (> 99%)
	2 (> 99%)		2 (> 99%)

Note: The long term periodicities marked with the symbol * do not appear in Fig. 1 due to the selected frequency scale.

periodicities, having in mind the different particle access from the interstellar medium in the inner heliosphere during periods with different polarity of the solar magnetic field. The appearance of some periods only in CR data, such as the 210 and 280 days and not in SFI ones indicates the different origin of the variations of this type.

Finally, the sunspot number, which is the most common tracer of solar activity, is not the only manifestation for solar induced effects in the interplanetary medium including the CR variations. The flare related parameters are also indicators of this modulation. This means, once again, that the investigation of CR variations provides a unique tool to derive information about the pattern of the interplanetary magnetic field and its flow as well as to determine the temporal and spatial evolution of their configurations. The CR intensity variations measured by neutron monitors is a mirror image of the magnitude of the IMF, as Cane et al. (1999) and Wang et al. (2000) have showed recently. The SFI as a mark of the energy emitted by the powerful flares could be regarded as a proxy data set to account for peculiar solar induced effects in the heliosphere. This connection between CR intensity variations recorded in different Neutron Monitor Stations with different cut-off rigidities and SFI should be very useful for Space Weather forecast purposes especially in our days that Neutron Monitor Stations provide CR data in "real-time".

Acknowledgements

We are grateful to Dr. R. Pyle and Dr. C. Lopate for helpful correspondence in providing cosmic ray data of Climax Neutron Monitor station and to Dr. T. Atac in kindly providing solar flare index data. Thanks are also due to the General Secretariat for Research and Technology supporting this work (Grant 70/4/6255 Greece-Russian Federation Joint Research and Technology Projects) and to the Special Research Account of Athens University for supporting this research.

References

Antalova, A., Kudela, K., Rybak, J., 2000. The variations of the solar activity and the low rigidity Comic Rays (1969–1998). ESA SP-463, 281.

Antalova, A., Kudela, K., Rybak, J., 2001. The solar and Comic Ray synodic periodicity (1969–1998). Space Science Reviews 97, 355.

Bai, T., 1994. The 51-day periodicity in cycle 22. Solar Physics 150, 385.

Bai, T., Cliver, E.W., 1990. A 154 day periodicity in the occurrence rate of proton flares. Astrophysical Journal 363, 299.

Blackman, R.E., Tukey, S.W., 1959. The Measurement of Power Spectra from the Point of View of Communications Engineering. Dover, New York.

Bouwer, S.D., 1992. Periodicities of solar irradiance and solar activity indices, II. Solar Physics 142, 365.

Cane, H.V., Wibberenz, G., Richardson, I.G., von Rosenvinge, T.T., 1998. Interplanetary magnetic field periodicity of ∼ 153 days. Journal of Geophysical Research 25, 4437.

Cane, H.V., Wibberenz, G., Richardson, I.G., von Rosenvinge, T.T., 1999. Cosmic ray modulation and the solar magnetic field. Geophysical Research Letters 26, 565–568.

Das, T.K., Nag, T.K., 1999. A 14-day periodicity in the mean solar magnetic field. Solar Physics 187, 177.

Das, T.K., Nag, T.K., Chatterjee, T.N., 1996. Short-term periodicity in proton fluences during solar cycle 22. Solar Physics 168, 385.

Kudela, K., Ananth, A.G., Venkatesan, D., 1991. The low-frequency spectral behaviour of cosmic ray intensity. Journal of Geophysical Research 96, 15871.

Kudela, K., Rybak, J., Antalova, A., Storini, M., 2002. Time evolution of low frequency periodicities in cosmic ray intensity. Solar Physics 205, 165.

Liritzis, I., Preka-Papadema, P., Petropoulos, B., Banos, C., Kostopoulos, T., 1999. Spectrum analysis of Jupiter's great red spot parameters: area, rotation, latitude and longitude (1963–1967). Planetary and Space Science 47, 469.

Mavromichalaki, H., Belehaki, A., Rafios, X., Tsagouri, I., 1997. Hale-cycle effects in cosmic-ray intensity during the last solar cycles. Astrophysics and Space Science 246, 7.

Mavromichalaki, H., Marmatsouri, E., Vassilaki, A., 1988. Solar cycle phenomena in cosmic-ray intensity: Differences between even and odd cycles. Earth, Moon and Planets 42, 233.

Mavromichalaki, H., Preka-Papadema, P., Petropoulos, B., Liritzis, I., Kurt, V., 2001. Possible influence of solar flares with hard X-ray emission on cosmic ray modulation, Proceedings of the Fourth Hellenic Astronomical Conference, Samos, p. 273.

Okhlopkov, V.P., Okhlopkova, L.S., Charakhch' yan, T.N., 1986. Annual cosmic-ray variations in the lower atmosphere. Geomagnetism and Aeronomy 26, 19–22.

Ozguc, A., Atac, T., 1989. Periodic behaviour of solar flare index during solar cycles 20 and 21. Solar Physics 123, 357.

Ozgüc, A., Atac, T., 1994. The 73-day periodicity of the flare index during the current solar cycle 22. Solar Physics 150, 339.

Rieger, E., Share, G.H., Forrest, O.J., Kanabach, G., Reppin, C., Chupp, E.I., 1984. A 154-day periodicity in the occurrence of hard solar flares? Nature 112, 623.

Rybak, J., Antalova, A., Storini, M., 2000. The intermittency of the solar intermediate-term periodicity (1969–1998). ESA SP-463, 419.

Rybak, J., Antalova, A., Storini, M., 2001. The wavelet analysis of the solar and cosmic-ray data. Space Science Reviews 97, 359.

Solar Geophysical Data, 1997. H.E. Coffey (ed.), NGDC/NOAA, Boulder, Colorado, 635 II.

Valdes-Galicia, J.F., Mendoza, B., 1998. On the role of large-scale solar photospheric motions in the cosmic-ray 1.68-yr intensity variation. Solar Physics 178, 1183.

Valdes-Galicia, J.F., Perez-Enriquez, R., Otaola, J., 1996. The cosmic-ray 1.68 year variation: a clue to understand the nature of the solar cycle?. Solar Physics 167, 409.

Valdes-Galicia, J.F., Caballero, R., Hurtado, A., 1999. 22 solar cycle cosmic ray intensity variations in the Mexico City Neutron Monitor, Proceedings of the 26th ICRC, Vol. 7. p. 119.

Verma, V.K., Joshi, G.C., Paliwal, D.C., 1992. Study of periodicities of solar nuclear gamma ray flares and sunspots. Solar Physics 138, 205.

Watari, S., 1996. Separation of periodic, chaotic and random components in solar activity. Solar Physics 168, 413.

Wang, Y.-M., Lean, J., Sheeley, N.R. Jr., 2000. The long-term variation of the Sun's open magnetic flux. Geophysical Research Letters 27, 505–508.

Wolff, C.L., 1992. Intermittent solar periodicities. Solar Physics 142, 187.

Xanthakis, J., Mavromichalaki, H., Petropoulos, B., 1989. Time evolution of cosmic-ray intensity modulation. Solar Physics 122, 345.

Yu-Qing, Lou., 2002. Rossby-type wave-induced periodicities in flare activities and sunspot areas or groups during solar maxima. Astrophysical Journal 540, 1102.